

Synthesis of portland cement clinker at low temperature using raw materials from western Mongolia

Rentsenkhand Magsarjav, Ochirkhuyag Bayanjargal, Khasbaatar Dashkhuu*

*Department of Chemical and Biological Engineering, National University of Mongolia, University Street 1,
Sukhbaatar district, Ulaanbaatar 14201, Mongolia*

**Authors to whom correspondence should be addressed:*

*Department of Chemical and Biological Engineering
National University of Mongolia, University Street 1
Sukhbaatar district, Ulaanbaatar 14201
Mongolia*

Email: d_khasbaatar@num.edu.mn

ORCID ID: <https://orcid.org/0000-0002-1311-1506>

This article has been accepted for publication and undergone full peer review but has not been through the copyediting, typesetting, and proofreading process, which may lead to differences between this version and the official version of record.

Please cite this article as: Magsarjav R., Bayanjargal O., Dashkhuu Kh. Synthesis of portland cement clinker at low temperature using raw materials from western Mongolia. *Mongolian Journal of Chemistry*, 27(55), 2026, xx-xx

<https://doi.org/10.5564/mjc.v27i55.4158>

Synthesis of portland cement clinker at low temperature using raw materials from western Mongolia

3

Rentsenkhand Magsarjav, <https://orcid.org/0009-0004-4438-3717>

Ochirkhuyag Bayanjargal, <https://orcid.org/0000-0003-0640-3313>

6

Khasbaatar Dashkhuu*, <https://orcid.org/0000-0002-1311-1506>

Department of Chemical and Biological Engineering, National University of Mongolia, University Street 1, Sukhbaatar district, Ulaanbaatar 14201, Mongolia

9

ABSTRACT

12 This study evaluates gypsum-assisted low-temperature synthesis of Portland cement clinker using limestone, marlstone, iron ore, and natural gypsum from Western Mongolia. A raw mix designed by Kind's method (LSF = 0.93; SM = 2.2) was sintered at 1100–1300 °C with 0–
15 2.0 wt.% gypsum addition, and replicated free-lime measurements were used to assess burnability. Increasing temperature markedly reduced residual free CaO, while moderate gypsum addition promoted CaO assimilation. Nonlinear regression identified, within the
18 investigated range, an optimum near 1.39 wt.% gypsum at 1300 °C, corresponding to a predicted free-lime content of approximately 1.25 wt.%. XRD and SEM confirmed the formation of an alite-rich clinker with developed silicate phases. Cement produced from this
21 clinker met the physical and mechanical requirements of MNS 0974:2008 for OPC 42.5 grade, confirming gypsum-assisted clinkerization as an effective route for promoting clinker phase formation at a reduced sintering temperature under the present experimental
24 conditions.

Keywords: Portland cement clinker, marlstone, iron ore, gypsum, XRD

27

30 © The Author(s). 2026 **Open access.** This article is distributed under the terms of the Creative Commons Attribution 4.0 International License (<https://creativecommons.org/licenses/by/4.0/>), which permits unrestricted use, distribution, and reproduction in any medium, provided you give appropriate credit to the original author(s) and the source, provide a
33 link to the Creative Commons license, and indicate if changes were made.

INTRODUCTION

The high-energy process of clinkering makes Portland cement, which is a key part of modern building construction. To make it, a finely ground homogeneous mixture of limestone and clay is heated to about 1400–1450 °C [1–4]. The high-temperature treatment breaks down carbonate raw materials and then makes the main clinker materials: alite ($3\text{CaO}\cdot\text{SiO}_2$ or C_3S), belite ($2\text{CaO}\cdot\text{SiO}_2$ or C_2S), tricalcium aluminate ($3\text{CaO}\cdot\text{Al}_2\text{O}_3$ or C_3A), and tetracalcium aluminoferrite ($4\text{CaO}\cdot\text{Al}_2\text{O}_3\cdot\text{Fe}_2\text{O}_3$ or C_4AF) [5, 6]. The density of the cement material is mostly due to the alite and belite that make up 70–80% of the clinker. To make the finished cement, cooled clinker is ground with a small amount of gypsum ($\text{CaSO}_4\cdot 2\text{H}_2\text{O}$), which is a set regulator that mostly affects the hydration rate of C_3A [7–9].

The clinkering process requires a lot of energy, especially for the endothermic breakdown of limestone and the formation of high-temperature phases. This is a big cost to the economy and the environment [10]. This is why a lot of research is going on around the world to find ways to make cement that are better for the environment and cheaper. Some strategies are to use industrial by-products or waste as alternative raw materials, use alternative fuels [11–13], improve clinker formation technologies [14], and, most importantly, add mineralisers or fluxing agents to the raw mix [1–4, 7, 8, 10, 11]. Mineralisers are substances that speed up the process of forming the clinker phase and/or lower the temperatures needed for the reaction, which saves energy [12]. Fluorides (e.g., CaF_2) [13, 15], sulphates, phosphates, and various oxides [16] have all been studied, but their use often comes with trade-offs. For example, fluorides may harm the environment, and some sulphates may change the mineralogy of clinker (e.g., belite stabilisation) [14–16]. Fluoride-sulfate mixtures, for example, have shown promise in lowering clinkering temperatures to around 1350 °C by forming intermediate phases. However, using them at the same time can be tricky [17].

Along with mineralisers that lower the temperature at which clinkering occurs, the larger field of cement and concrete technology uses a lot of other additives and admixtures that change properties for certain uses. Blast furnace slag (BFS) and pulverised fly ash (PFA) are two examples of supplementary cementitious materials that are often used as partial replacements for clinker. This lowers the overall CO_2 burden and usually makes the material more durable and resistant to chemicals in the long term [18, 19]. Low-dosage superplasticizers (about 1%) are chemical additives that make concrete easier to work with and use less water by making it denser and stronger [20]. Adding latexes or polymerisation in place to polymers changes the microstructure, which makes the cement stronger, stickier, and more water-resistant [21–23]. These different types of additives improve many different

parts of how the cement and concrete work. However, the mineralisers are only meant to
69 make the energy-intensive part of the clinkering process better.

Gypsum ($\text{CaSO}_4 \cdot 2\text{H}_2\text{O}$), which is usually used to slow down the setting of cement, has also
been studied as a mineraliser for making clinker. Adding gypsum seems to help the
72 formation of intermediate phases like $\text{C}_4\text{A}_3\text{SO}_3$ (calcium sulfoaluminate) and may also speed
up the formation of alite and belite at lower temperatures [24–28]. Some studies say that
gypsum may have some bad effects, like making belite more stable [7, 9, 10], but it is a
75 better choice for the environment than fluoride-based mineralisers [24, 25].

Limestone, marlstone, iron ore, and gypsum are just a few of the many raw materials found
in western Mongolia that can be used to make cement [29]. Using these local materials
78 could help the region grow and make it less reliant on imported cement. So, it is very
important to make the production process as energy-efficient as possible. The goal of this
study is to see if it is possible to make Portland cement clinker at lower temperatures by
81 mixing limestone and marlstone from the Khovd and Uvs aimags in Western Mongolia with
iron ore from the same area and using gypsum from the Baruuntserd deposit as a
mineraliser. The present study concentrates on the characterisation of raw materials, the
84 identification of an optimal raw mixture and gypsum dosage via systematic experimentation
and modelling, the synthesis of clinker at reduced temperatures, and the evaluation of the
properties of the resulting cement in relation to established standards.

87 **EXPERIMENTAL**

Materials

The raw materials utilised in the current study were sourced from the western region of
90 Mongolia. The limestone came from a deposit about 11 km southeast of the Khovd aimag
center ($47^\circ 56' 21''$ – $47^\circ 56' 28''$ N, $91^\circ 15' 15''$ – $91^\circ 15' 30''$ E). The marlstone came from a deposit
that is about 14 km east of Sagil sum in Uvs aimag ($50^\circ 25' 67''$ N, $91^\circ 46' 21''$ E). The iron ore
93 used as the fluxing agent came from the Kharganat deposit, which is about 45 km northwest
of Naranbulag sum, Uvs aimag (coordinates: $49^\circ 37' 00''$ N, $92^\circ 11' 00''$ E). The mineraliser
was natural gypsum that came from the Baruuntserd deposit, which is about 14 km east of
96 Sagil sum, Uvs aimag, near the Baruun Tagna Mountain (coordinates: $50^\circ 25' 20''$ N,
 $91^\circ 44' 23''$ E).

Material characterization methods

99 *X-ray fluorescence analysis:* The Axios MAX instrument with a 4-kW X-ray tube was used to perform wavelength dispersive X-ray fluorescence (XRF) spectrometry on powdered samples to determine the chemical compositions of all the raw materials.

102 *X-ray diffraction analysis:* We used a MAXimaX7000 diffractometer with Cu-K α radiation at 40 kV and 30 mA to record XRD diffractograms. We took data over a 2θ range of 5–60° with a step size of 0.02° and an integration time of 0.6 s per step. We used Match! software
105 (Crystal Impact, Germany) to find the phases, and then we used X'Pert HighScore Plus (Malvern Panalytical, The Netherlands) to check the peak indexing and reference-pattern verification. The XRD results were used to figure out what phases were present and to get
108 a rough idea of how much of each major clinker phase was present.

Thermal analysis: A Derivatograph T-1500 (Hungary) thermoanalyzer was used to determine thermal analysis (TG/DTA). A heating rate of 10 °C/min to a suitable final
111 temperature (implicitly sufficiently elevated for decomposition reactions, e.g., >800 °C for the decomposition of carbonates or dehydration of gypsum) in an air stream utilizing the reference material α -Al₂O₃.

114 **Designing and calculating the raw mix**

We used Kind's method [29] to figure out the oxide compositions of the individual raw materials using XRF analysis. The main goal of the raw mix design was to get a chemical
117 makeup that was similar to OPC clinker while making sure it could be burnt at lower clinkering temperatures.

We chose two compositional moduli as design goals: the lime saturation factor (LSF = 0.93)
120 and the silica modulus (SM = 2.2). These values are in the normal range for OPC clinker and were chosen on purpose to make sure there is enough CaO available for alite formation while reducing the risk of too much free lime, which is more important at lower firing
123 temperatures. The chosen SM value also makes sure that there is a good balance between silicate and interstitial phases, which helps melt form and speeds up the process of making clinker.

126 We found the mass fractions of limestone (x_L), marlstone (x_M), and iron ore (x_I) by solving a system of simultaneous equations that included:

(i) a mass balance constraint,

129

$$x_L + x_M + x_I = 1$$

(ii) the target silica modulus,

$$SM = \frac{SiO_2}{Al_2O_3 + Fe_2O_3}$$

132 and
 (iii) the target lime saturation factor,

$$LSF = \frac{CaO}{2.8SiO_2 + 1.2Al_2O_3 + 0.65Fe_2O_3}$$

135

In this approach, the oxide composition of the raw mix was calculated as a weighted average of the corresponding oxide contents of each raw material, using their respective mass fractions.

138

To evaluate the potential clinker phase assemblage associated with the designed raw mix, classical Bogue calculations were applied to the clinker-normalized oxide composition.

141

Prior to the calculation, the raw mix oxide contents were converted to a clinker basis by normalization to a loss-on-ignition-free condition. The Bogue method assumes complete reaction and thermodynamic equilibrium and was employed as a theoretical tool to estimate the relative proportions of the major clinker phases.

144

The phase contents (in wt%) were calculated using the following standard Bogue equations:

147

- Tetracalcium aluminoferrite (C_4AF):

$$C_4AF = 3.043 \times Fe_2O_3$$

150

- Tricalcium aluminate (C_3A):

$$C_3A = 2.650 \times Al_2O_3 - 1.692 \times Fe_2O_3$$

153

- Tricalcium silicate (C_3S):

$$C_3S = 4.071 \times CaO - 7.602 \times SiO_2 - 6.718 \times Al_2O_3 - 1.430 \times Fe_2O_3$$

156

- Dicalcium silicate (C_2S):

$$C_2S = 2.867 \times SiO_2 - 0.754 \times C_3S$$

159

The Bogue calculation was used as a theoretical verification tool to assess whether the designed raw mix chemistry is consistent with OPC clinker, while recognizing that the actual phase assemblage may differ due to kinetic limitations and the presence of minor

162

components.

Clinker synthesis

The oxidation reaction was performed in a thermostatted oil bath using a round-bottom flask. The catalyst was pre-swollen in acetonitrile (20 ml) for 30 minutes before adding ethylbenzene (10 mmol), an oxidant (20 mmol), and the catalyst (0.1–0.15 g). The mixture was refluxed and the reaction was primarily examined on TLC under the varying conditions such as catalyst amount, oxidant type (TBHP, H₂O₂), temperature, and duration (4–8 h). The products were confirmed by GC-MS.

Clinker and Cement Characterization

The efficiency of the process of sintering and the role of the added gypsum and temperature were mainly evaluated by measuring the amount of residual free lime (CaO_{free}) in cooled clinkers. This measurement was carried out with a rapid method of volumetric titration [30, 31]. The composition of the selected synthesized clinkers under the identified optimal conditions was obtained from XRD. The microstructural analysis of the clinkers was conducted with a scanning electron microscope (SEM; Hitachi TM-1000, Hitachi High-Technologies Corporation, Tokyo, Japan).

The synthesized clinkers were ground with an optimized gypsum amount and formed into samples. The amount of gypsum used was determined by the analysis of SO₃ for setting time control [32]. Physical and mechanical properties of the resultant cements were assessed following standard practices. Specific surface area was assessed with a Blaine air permeability apparatus (Zhejiang, DBT-127). Water demand for normal consistency and setting times were determined by Vicat apparatus (Relaible, IS: 5513). Compressive strength of mortar specimens for the appropriate curing ages was evaluated using a compression testing machine (Zhejiang, STYE-300).

Experimental optimization

The following mathematical modeling process with the use of multidimensional nonlinear regression was employed as a tool in identifying the best conditions for the synthesis of the clinker within the investigated range of experiments. The added gypsum amount (X₁) and the burning temperature (X₂) acted as the independent variables, and the obtained free lime amount (y) as the response (dependent variable). MATLAB software was used in the analysis with the aim of determining the optimum combination of gypsum percent and temperature that gives the lowest amount of free lime, reflecting the most thorough clinkerization reaction.

RESULTS AND DISCUSSION

Raw material characterization

198 The samples of raw materials obtained from Western Mongolia as potential raw materials for Portland cement production were assessed by chemical and mineralogical analysis. Table 1 shows the chemical compositions obtained using XRF.

Table 1. Chemical compositions of raw materials, (w. %)

No	Oxides	Ls ^a	Ms ^b	K.I.O. ^c	G.B. ^d
1	SiO ₂	0.6	32.02	7.06	2.34
2	Al ₂ O ₃	0.23	6.7	1.02	0.72
3	Fe ₂ O ₃	0.16	2.66	89.2	0.44
4	CaO	55.24	26.03	0.53	32.2
5	MgO	0.26	1.49	-	0.28
6	Na ₂ O	0.1	0.89	1.02	0.21
7	K ₂ O	0.1	1.37	1.02	0.08
8	SO ₃	0.1	3.06	0.15	41.6
9	MnO	0.022	0.152	-	
10	P ₂ O ₅	0.02	0.103	-	
11	TiO ₂	0.017	0.378	-	
12	Mn ₂ O ₃	-	-	-	
13	Others	-	6.577	0.01	0.22
14	LOI	43.17	18.57	-	21.91
15	Σ	100.009	100	100	100

Note: ^aLimestone, ^bMarlstone, ^cKharganat iron ore, ^dGypsum of Baruuntserd

Table 2. Minerals in raw materials, (%)

No	Mineral name	Mineral formula	Int.mineral abbreviation	Limestone	Marlstone	Kharganat iron ore	Baruuntserd Gypsum
1	Calcite	CaCO ₃	Cal	98.8	33.1		1.93
2	Quartz	SiO ₂	Qz	1.2	19.7	9.56	
3	Gypsum	Ca(SO ₄)·2H ₂ O	Gp		18.7		96.25
4	Albite	NaAlSi ₃ O ₈	Ab		7.5		
5	Kaolinite (phyllosilicate)	Al ₂ (Si ₂ O ₅)·(OH) ₄	Kln		6.2		
6	Muscovite	KAl ₂ (Si ₃ Al)O ₁₀ (OH) ₄	Ms		14.8		
7	Hematite	Fe ₂ O ₃	Hem			13.78	
8	Magnetite	Fe ₃ O ₄	Mag			44.25	
9	Andradite	Ca ₃ Fe ₂ (SiO ₄) ₃	Adr			32.42	

204 The Uvs marlstone presented a more complex composition, containing significant amounts of SiO₂ (32.02%), Al₂O₃ (6.7%), and CaO (26.03%), along with minor amounts of Fe₂O₃, MgO, and alkalis (Na₂O, K₂O). Its LOI was 18.57%. XRD analysis (Figure 1 (b), Table 2)
 207 revealed a mixed mineralogy for the marlstone, including calcite (33.1%), quartz (19.7%), gypsum (18.7%), albite (7.5%), kaolinite (6.2%), and muscovite (14.8%). The composition of the marlstone containing the required silica and alumina components for the production
 210 of a clinker classifies it as an argillaceous or siliceous corrective material.

The Kharganat iron ore used as a flux contained iron oxides with 89.2% Fe₂O₃ as per XRF (Table 2). From XRD analysis (Figure 1(c), Table 1), the primary iron-carrying phase is revealed as the magnetite (Fe₃O₄, 44.25%), with the second phase being the hematite (Fe₂O₃, 13.78%) and andradite (Ca₃Fe₂(SiO₄)₃, 32.42%), proving its potential as an iron carrier for the development of a melt.

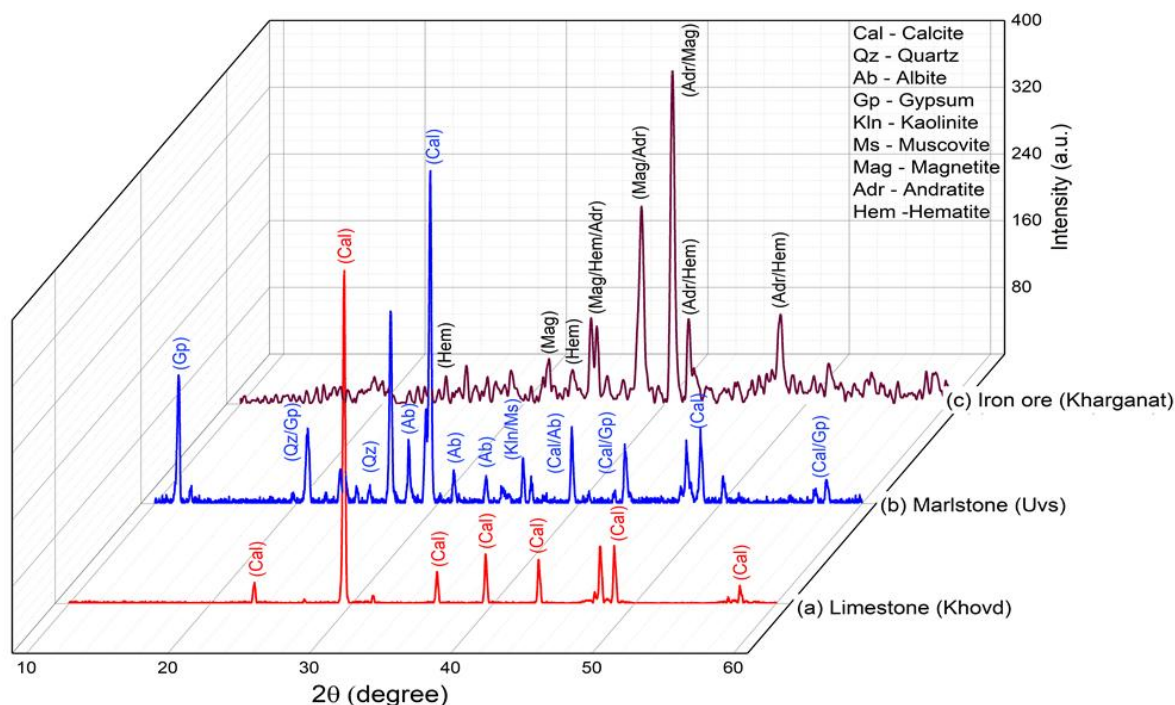


Fig. 1. XRD patterns of (a) Limestone (Khovd), (b) Marlstone (Uvs), (c) Iron ore (Kharganat)

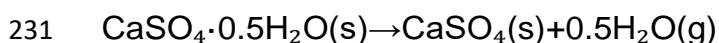
The Baruuntserd gypsum was characterized by TG/DTA (Figure 2), which was used first as a mineraliser and then as a set regulator. The two-step dehydration process that took place at 130 °C and 185 °C caused a weight loss of 20.2%, which made it possible to figure out that the CaSO₄·2H₂O content was 96.25%. The thermal breakdown of CaSO₄·2H₂O usually happens in two steps of dehydration:

1. The first step in dehydration (making hemihydrate) is:

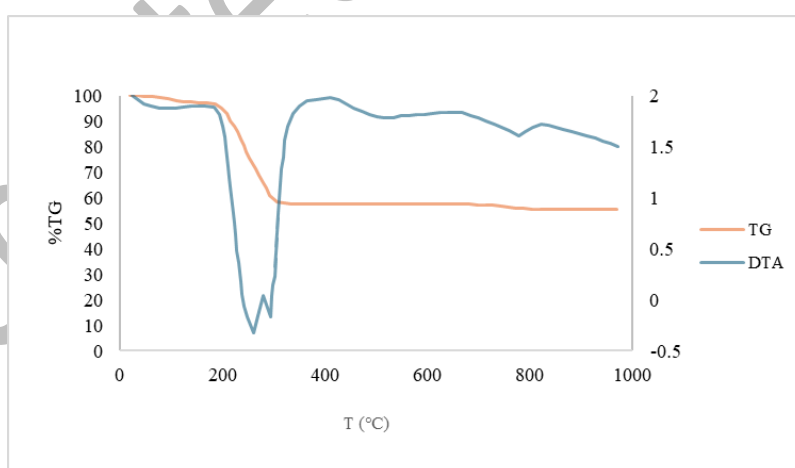


The first dehydration, which is the loss of 1.5 molecules of water, shows up on the TG curve as a big weight loss that happens between 100 °C and 150 °C, with a bigger drop around 130 °C. The DTA curve shows a sharp endothermic peak in this temperature range. This confirms that energy is being absorbed when water molecules are removed to make calcium sulphate hemihydrate.

2. Second Dehydration Step (Making Anhydrite):



The second step in the dehydration process is to take away the last 0.5 molecules of water from the hemihydrate. This makes anhydrous calcium sulphate (anhydrite). The TG curve shows this change by showing a further, often sharper, weight loss between 150 °C and 200 °C, with a clear drop around 185 °C. In this temperature range, the DTA curve shows a second, usually larger, endothermic peak. This means that more energy is needed to completely remove the water. The information says that the total weight loss was 20.2%. This experimental value is very close to the theoretical total weight loss of 20.93% for pure $\text{CaSO}_4 \cdot 2\text{H}_2\text{O}$. The small difference could be because of small impurities in the sample or differences in the experiment. The $\text{CaSO}_4 \cdot 2\text{H}_2\text{O}$ content was found to be 96.25% based on the weight loss, which shows that the Baruuntserd gypsum sample is very pure. A small peak in decarbonation around 740 °C showed that there was a small amount of calcite (1.93%). Because the gypsum is very pure, it works well for what it is meant to do. The endothermic effects seen at 500 °C and 800 °C happen without losing a lot of mass, as shown by the flat TG curve. This shows that these are not reactions that break things down. Solid-state phase transitions are what cause them instead. At about 500 °C, β -anhydrite changes into α -anhydrite, which is a polymorphic transformation. The smaller dip at around 800 °C probably means that the structure of the anhydrite crystal has changed slightly again [33].



252 **Fig. 2.** DTA/TG curves of Baruuntserd gypsum

Overall, the chemical compositions of the limestone, marlstone, and iron ore were deemed appropriate for formulating a Portland cement raw mix.

255 **Raw mix design and clinker synthesis optimization**

Using the target values of LSF = 0.93 and SM = 2.2, the mass fractions of limestone (x_L), marlstone (x_M), and iron ore (x_I) were determined through Kind's method. Each oxide content of the raw mix (Mix-A) was calculated as a weighted average of the corresponding oxide contents of the individual raw materials, using their respective mass fractions. The resulting raw mix and clinker-normalized oxide compositions are summarized in Table 3.

As an illustrative example of the calculation procedure, the silica content of the raw mix ($SiO_{2,mix}$) was determined using the weighted-average approach:

$$SiO_{2,mix} = x_L \cdot SiO_{2,L} + x_M \cdot SiO_{2,M} + x_I \cdot SiO_{2,I}$$

Substituting the calculated mass fractions and XRF-measured oxide contents yields:

$$SiO_{2,mix} = 0.5621 \times 0.60 + 0.4140 \times 32.02 + 0.0239 \times 7.06 = 13.76 \text{ wt\%}$$

This value represents the silica content of the raw mix prior to decarbonation and was subsequently converted to a clinker basis by normalization to a loss-on-ignition-free condition. The same calculation procedure was applied to all other major oxides, as reported in Table 3.

Table 3. Result of raw mix calculations (%)

<i>Chemical composition</i>			
No	Oxide	<i>Raw mix composition</i>	<i>Clinker composition</i>
1	SiO ₂	13.76	20.23
2	Al ₂ O ₃	2.93	4.30
3	Fe ₂ O ₃	3.32	4.88
4	CaO	41.84	61.50
5	MgO	0.76	1.12
6	Na ₂ O	0.45	0.66
7	K ₂ O	0.65	0.95
8	SO ₃	1.33	1.95
9	MnO	0.08	0.11
10	P ₂ O ₅	0.05	0.08
11	TiO ₂	0.17	0.24
12	Others	2.72	4.00
13	LOI	31.95	-
14	Total	100.01	100.02
<i>Phase composition</i>			
1	C ₃ S		60.73
2	C ₂ S		12.18
3	C ₃ A		3.12
4	C ₄ AF		14.84
5	Ls ^a	56.21	
6	Ms ^b	41.40	
7	H.I.O ^c	2.39	
8	Σ	100	100

Note: C₃S- alite, C₂S- belite, C₃A- aluminate, C₄AF- [tetra-calcium aluminoferrite](#).
^{a)} Limestone, ^{b)} Marlstone, ^{c)} Kharganat iron ore

273 The clinker-normalized oxide composition derived from the optimized raw mix lies
 within the typical compositional envelope of OPC clinker. Based on this composition,
 Bogue phase calculations (Table 3) indicate an alite-rich clinker, accompanied by
 276 moderate amounts of belite and interstitial phases. Although the Bogue method
 provides an idealized equilibrium-based estimation, the calculated phase assemblage
 offers a robust chemical framework for interpreting the clinker formation behavior
 279 observed experimentally.

In addition to oxide and phase compositions, Table 3 also presents the calculated
 mass fractions of the three raw materials—limestone (56.21 wt%), marlstone (41.40
 282 wt%), and iron ore (2.39 wt%)—used in the present study. Limestone serves as the
 primary source of CaO, marlstone supplies the majority of SiO₂ together with a
 significant portion of Al₂O₃, and the iron ore addition, despite its low proportion, plays
 285 a critical role in adjusting the Fe₂O₃ content and promoting liquid-phase formation
 during clinkerization.

Overall, the optimized raw material proportions, clinker-normalized oxide composition,
 288 and Bogue-based phase estimations indicate that the designed raw mix is chemically
 balanced and suitable for systematically evaluating the combined effects of gypsum
 addition and firing temperature on clinker formation behavior, phase evolution, and
 291 burnability under the present experimental conditions.

Effect of gypsum addition and temperature on free lime content and optimization of clinkerization conditions

294 To evaluate the mineralizing effect of gypsum on clinker formation, the base raw mix
 (Mix A), designed using Kind's method, was modified by incorporating different
 amounts of natural gypsum from the Baruuntserd deposit. Four compositions were
 297 prepared: a control mix without gypsum (A1) and three gypsum-bearing mixes
 containing 1.0 wt.% (A2), 1.5 wt.% (A3), and 2.0 wt.% (A4) gypsum, calculated relative
 to the initial raw mix mass (Table 4).

300 **Table 4.** Composition of raw material mixture (%)

Mix	Mix-A ₁	Mix-A ₂	Mix-A ₃	Mix-A ₄
Initial mix percentage	100	99.0	98.5	98.0
Added gypsum amount, %	=	1.0	1.5	2.0

Note: Mix-A₁, without gypsum, Mix-A₂ 1.0 percent of gypsum, Mix-A₃ with 1.5 percent of gypsum Mix-A₄ with 2.0 percent of gypsum

303

All raw mixes were homogenized, briquetted, and sintered at three temperatures, namely 1100, 1200, and 1300 °C, using a constant holding time of 45 min. A total of 36 clinker

306 samples were produced, covering four gypsum addition levels and three temperature conditions with replicated experiments for each case. The reported free lime (CaO_{free}) values are presented as mean standard deviation of the replicated measurements.

309 The degree of clinkerization was primarily assessed by determining the residual free lime content (CaO_{free}) of the fired samples, as free lime is a sensitive indicator of reaction completeness and burnability. The measured CaO_{free} values for all experimental conditions are summarized in Table 5. As expected, a general decrease in free lime content was observed with increasing firing temperature, while gypsum addition further enhanced CaO assimilation within the investigated range.

315

Table 5. Residual free lime (CaO_{free}) contents of clinkers synthesized at different gypsum additions and sintering temperatures

Name of Mix	Added, (%)	CaO _{free}		
	CaSO ₄ * 2H ₂ O	1100 °C	1200 °C	1300 °C
Mix-A ₁	0.0	23.49 ± 0.52	16.10 ± 0.07	7.88 ± 0.82
Mix-A ₂	1.0	21.12 ± 1.36	12.56 ± 0.79	4.79 ± 2.62
Mix-A ₃	1.5	18.13 ± 0.89	7.98 ± 0.07	2.68 ± 0.01
Mix-A ₄	2.0	23.98 ± 0.35	18.08 ± 0.18	10.85 ± 0.18

318

Gypsum (CaSO₄·2H₂O) acts as a mineralizer in clinkerization by influencing key mechanisms that improve clinker quality at lower temperatures [34, 35]. It lowers the temperature for liquid phase formation, creating a molten phase that enhances mass transport and accelerates reactions between raw materials, promoting better assimilation of calcium oxide (CaO) into clinker phases. Gypsum also promotes the formation of alite (C₃S), the primary phase responsible for early strength in OPC, by enhancing CaO reactivity and facilitating intermediate phase formation. Additionally, sulfates stabilize belite (C₂S), contributing to later strength development. At 1300 °C, transient sulfate phases such as alkali sulfates, calcium langbeinite, and calcium sulfoaluminates (ye'elinite) form. These phases promote liquid formation, enhance ion mobility, and act as temporary reservoirs for sulfur and aluminum, facilitating their controlled incorporation or release during clinkering. Sulfates also catalyze clinker phase formation, speeding up free lime assimilation and crystallization of clinker minerals [36].

To quantitatively analyze the combined influence of gypsum dosage and sintering temperature on free lime content, mathematical modeling based on multidimensional nonlinear regression was applied. In the regression analysis, the normalized independent variables were defined as follows: the gypsum content was expressed as:

333

$$x_1 = \frac{(\text{gypsum wt.\%} - 1.5)}{0.5},$$

336 and the burning temperature as:

$$x_2 = \frac{(T - 1200)}{100},$$

339 where T is the sintering temperature in °C. The response variable y corresponds to the measured free lime content (CaO_free, wt.%).

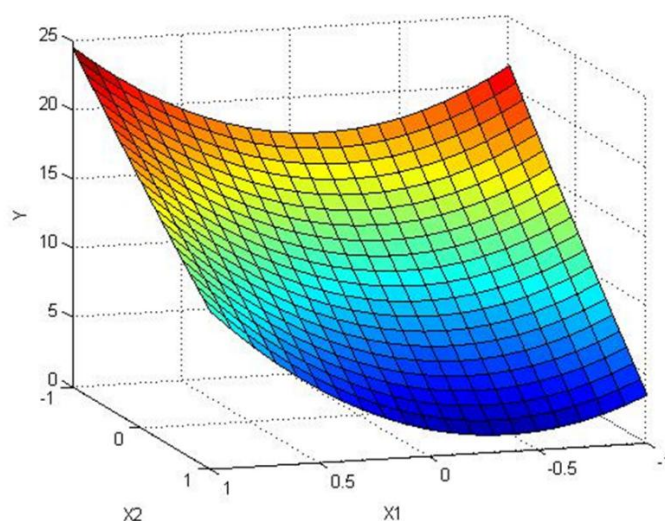
A second-order polynomial regression model with interaction terms was selected to describe
342 the system:

$$y = b_0 + b_1x_1 + b_2x_2 + b_3x_1x_2 + b_4x_1^2 + b_5x_2^2.$$

The regression coefficients (b_0 – b_5) were determined using MATLAB software based on the
345 experimental data set. The resulting regression equation is given as:

$$y = 9.4874 + 2.6267x_1 - 7.787x_2 + 1.168x_1x_2 + 5.4993x_1^2 + 0.2153x_2^2.$$

The average value of the response variable was calculated as $M(y) = 13.11$. The relative
348 error of the regression model was 3.9%, corresponding to a model confidence of approximately 96.2%, indicating good agreement between the experimental and predicted values. The three-dimensional response surface generated from the regression equation is
351 presented in Figure 3. The surface illustrates the predicted trend of decreasing free lime with increasing temperature and moderate gypsum addition within the investigated experimental range. The minimum region indicates the condition selected for further experimental
354 validation.



357 **Fig. 3.** Three-dimensional response surface showing the effect of gypsum content and sintering temperature on free lime

To find the best amount of gypsum to use at the highest temperature studied, the sintering temperature was set at 1300 °C ($x_2 = 1$), and the partial derivative of the regression function with respect to x_1 was set to zero:

$$\frac{\partial y}{\partial x_1} = 0.$$

Solving this condition gave an optimal value of $x_1 = -0.226$, which meant adding about 1.39 ± 0.01 wt.% of gypsum. At this point, the expected lowest amount of free lime was $y \approx 1.25 \pm 0.07$ wt.%.

Thus, within the examined experimental parameters, the condition of approximately 1.39 ± 0.01 wt.% gypsum addition and a sintering temperature of 1300 °C was determined to be the optimal clinkerization condition for reducing residual free lime. Based on this result, Mix A with 1.39 ± 0.01 wt.% gypsum was used to make clinker and then analysed in detail for its phases and microstructure. It was sintered at 1300 °C for 45 minutes.

Characterisation of clinker

The three clinker samples made under the identified optimum condition within the investigated range (1.39 ± 0.01 % gypsum addition, sintering at 1300 °C for 45 min) were further tested. To confirm the reproducibility of the experimental results, independently prepared clinker samples were synthesised under identical conditions and subjected to analysis. Samples showed stable phase assemblages and microstructural characteristics within the limits of experimental uncertainty, which confirmed that the results were accurate.

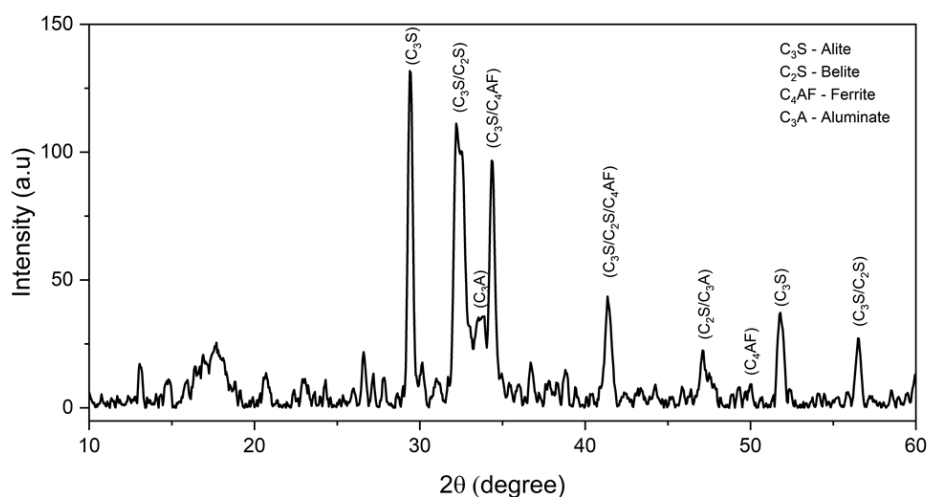
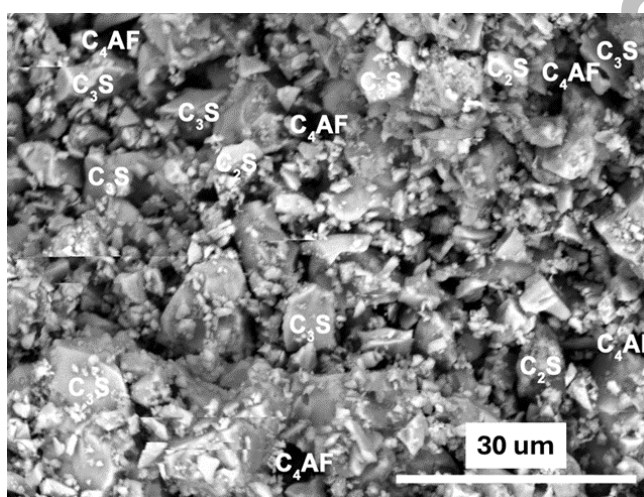


Fig. 4. XRD pattern of clinker synthesized at 1300 °C for 45 min with 1.39 wt.% gypsum addition. The labelled peaks correspond to the main Portland cement clinker phases: C_3S = alite, C_2S = belite, C_3A = tricalcium aluminate, and C_4AF = tetracalcium aluminoferrite.

381 X-ray diffraction (XRD) analysis (Figure 4) confirmed the formation of the major Portland
cement clinker phases. Semi-quantitative interpretation of the XRD pattern suggested that
the clinker was predominantly composed of alite (~61%), together with belite (~24%),
384 tricalcium aluminate (~7%), and tetracalcium aluminoferrite (~8%).

The relatively high alite content classifies this clinker as alite-rich, which is generally
associated with favorable early strength development [3]. The observed belite content is
387 higher than the value predicted by the Bogue calculation (12.18%), which may be attributed
to the reduced sintering temperature and the presence of sulfate species originating from
gypsum addition, as sulfates are known to partially stabilize belite formation [11, 18, 20].
390 Nevertheless, the substantial alite formation confirms the effectiveness of gypsum-assisted
low-temperature clinker synthesis under the present experimental conditions.



393 **Fig. 5.** Morphology of clinker prepared by optimal condition. White labels indicate the main
microstructural features: C₃S = alite crystals, C₂S = belite grains, C₄AF = interstitial aluminoferrite
396 phase

Scanning electron microscopy (SEM) was used to examine the microstructure of the clinker
synthesized under the identified optimal conditions (Figure 5). The SEM image shows a
399 well-developed clinker microstructure dominated by silicate phases with interstitial
aluminoferrite phases. Alite (C₃S) appears as large, angular to subhedral prismatic and
plate-like crystals, typical of well-crystallized alite reported for Portland cement clinker [37].
402 Rounded to sub-rounded belite (C₂S) grains are observed adjacent to and partially
embedded within the alite matrix, consistent with typical belite morphology and supporting
the XRD results indicating a higher C₂S content than predicted by Bogue calculations [38].
405 C₄AF mostly fills the spaces between the silicate grains in the interstitial regions. This makes
darker, irregular to prismatic phases that fill the spaces between the grains. This suggests
that there was a temporary liquid phase during clinkerization. The observed microstructure
408 is consistent with effective phase development, low free lime content, and the XRD-identified

phase assemblage, indicating successful clinkerization at 1300 °C under the present experimental conditions.

411 **Cement properties**

The physical and mechanical properties of the cements produced from the optimized low-temperature clinkers were evaluated and compared with those of commercial ordinary
414 Portland cements and the requirements of the Mongolian standard MNS 0974:2008 [39] (Table 6). The consistency values for synthesised cements are 27.30 ± 0.14 %, which is in the same range as commercial OPCs (0.263 ± 0.003 %). This indicates that the cements
417 behave like normal cement. The water-to-cement ratios needed to get standard consistency are similar to those of reference cements. This shows that making clinker at a lower temperature does not change the amount of water needed.

420 **Table 6.** Physical characteristics of cement

№	Cement Samples	Normal consistency	Water/cement ratio	t_s^a , hour		Specific surface area, m ² /kg
				t_i^b	t_f^c	
1	Khutul	27.9	1: 0.268	2.25	3.5	407.8
2	Ulaan	28.6	1: 0.279	2.40	3.55	465
3	Nalgar tushig	26.7	1: 0.262	2.40	3.55	463
4	Mix-Opt	27.30 ± 0.14	$1: 0.263 \pm 0.003$	2.385 ± 0.024	3.51 ± 0.01	400.0 ± 2.83
6	OPC ^d	≥ 24.0	1: 0.260	> 0.67	< 10	> 300

Note: ^a setting time, ^b initial setting time, ^c final setting time, ^d Standard of ordinary Portland cement- MNS 0974 :2008

423 **Table 7.** Mechanical characteristics of cement

№	Cement Samples	Tensile/Flexural strength, MPa		Compressive strength, MPa	
		3 day	28 day	3 day	28 day
1	Khutul	4.70	8.07	18.17	42.73
2	Ulaan	5.20	8.20	19.33	43.10
3	Nalgar tushig	5.87	7.87	26.03	45.60
4	Mix-Opt	5.34 ± 0.03	7.99 ± 0.04	20.15 ± 0.40	42.95 ± 0.35
6	OPC ^d	≥ 3.5	≥ 6.5	≥ 17.0	≥ 42.5

Note: ^d Standard of ordinary Portland cement- MNS 0974 :2008

Setting time results further confirm the suitability of the synthesized cements. Initial setting
426 times of 2.385 ± 0.024 h and final setting times of 3.51 ± 0.01 h comply with standard limits and closely match those of commercial products, indicating effective regulation of aluminate hydration by the optimized gypsum addition during grinding. The specific surface areas
429 (400.0 ± 2.83 m²/kg) exceed the minimum standard requirement (>300 m²/kg) and are comparable to commercial cements, with minor differences attributed to grinding efficiency rather than clinker quality. Mechanical performance shows (Table 7) that synthesized
432 cements satisfy the OPC 42.95 ± 0.35 grade requirements. The 3-day compressive strengths (20.15 ± 0.40 MPa) exceed the minimum standard value, while 28-day strengths

of 42.95 ± 0.35 MPa confirm that long-term strength development is not compromised by
435 the reduced clinkering temperature. This behavior is consistent with the alite-rich phase
composition and dense clinker microstructure observed by XRD and SEM. In general, the
similar physical properties and mechanical performance of Mix-Opt show that clinker made
438 at 1300 °C under the best conditions can make cement that meets standards. This supports
the idea that gypsum-assisted low-temperature clinkerization is a promising route for cement
production that uses less energy.

441

CONCLUSIONS

444 Within the experimental domain examined in this study, Portland cement clinker was
successfully synthesized at 1300 °C using limestone, marlstone, iron ore, and natural
gypsum from Western Mongolia. Chemical and mineralogical characterization confirmed
that these raw materials can be proportioned into a chemically balanced OPC-type raw mix
447 by Kind's method, with target values of LSF = 0.93 and SM = 2.2.

Replicated sintering experiments conducted over 0–2.0 wt.% gypsum addition and 1100–
1300 °C showed that increasing temperature was the primary factor enhancing
450 clinkerization, while moderate gypsum addition further promoted CaO assimilation.
Nonlinear regression analysis identified an optimum near 1.39 wt.% gypsum at 1300 °C
within the investigated range, corresponding to a predicted residual free CaO content of
453 approximately 1.25 wt.%. Therefore, this condition should be interpreted as optimal only
under the present experimental conditions, not as a universal optimum.

XRD and SEM observations indicated the formation of an alite-rich clinker containing C_3S ,
456 C_2S , C_3A , and C_4AF , with developed silicate crystals and interstitial aluminoferrite phases.
Cement produced from this clinker exhibited normal consistency, setting times, Blaine
fineness, and compressive strength values satisfying MNS 0974:2008 requirements for
459 OPC 42.5 grade, with performance comparable to commercial Portland cements.

AUTHOR CONTRIBUTIONS

The contributions of the authors to this research are as follows: RM: Participated in the
conceptualization of the research; conducted the experimental work; curated the data;
contributed to the drafting of the manuscript: OB: Conceptualized and designed the overall
research; supervised the research project, curated the data; performed preliminary data
processing: KhD: Defined the research methodology; performed data analysis of the
experimental results; reviewed and edited the manuscript; supervised the research project.
All authors have read and approved the final version of the manuscript for publication.

CONFLICT OF INTEREST

The authors declare that they have no known competing financial interests or personal relationships that could have appeared to influence the work reported in this paper. All authors are affiliated with the National University of Mongolia, and this affiliation does not present a conflict of interest regarding the publication of this research.

ACKNOWLEDGEMENTS

The research reported in this paper was supported by the "Functional materials based on Mongolian natural minerals for environmental engineering, cementitious and flotation processes" project (J11A15) under the Higher Engineering Education Development (M-JEED) Project.

REFERENCES

1. Kamitsou M.D., Kanellopoulou D.G., Christogerou A., et al. (2022) "A Contribution towards a More Sustainable Cement: Synergy of Mill Scales, Greek Wet Fly Ash, Conventional Raw Materials and Clinkering Temperature," *Minerals*, vol. 12, no. 324
462 <https://doi.org/10.3390/min12030324>
2. Soomro M., Tam V.W.Y., Jorge Evangelista A.C., (2023) "Production of cement and its environmental impact," *Recycled Concrete*, p. 11–46.
465 <https://doi.org/10.1016/B978-0-323-85210-4.00010-2>
3. Zhanikulov N., Sapargaliyeva B., Agabekova A., et al. (2023) "Studies of Utilization of Technogenic Raw Materials in the Synthesis of Cement Clinker from It and Further Production of Portland Cement," *Journal of Composites Science*, vol. 7, no. 226.
468 <https://doi.org/10.3390/jcs7060226>
4. Scrivener K.L., Snellings R., (2022) "The Rise of Portland Cements," *Elements*, vol. 18, p. 308–313. <https://doi.org/10.2138/gselements.18.5.308>
471
5. Kim T., Kim Y., Kim N., Seo J., Cho J (2024) "Production of High-Strength Cement Clinker Using Slag-Based Industrial By-Products," *Resources Recycling*, vol. 33, p. 64–74.
474 <https://doi.org/10.7844/kirr.2024.33.6.64>
6. Fu J., Guo W., Hu Y., et al. (2024) "Synthesis and properties of belite-ye'elimite-ternesite cement clinker at 1200 °C," *Journal of Sustainable Cement-Based Materials*, vol. 13, p. 968–977. <https://doi.org/10.1080/21650373.2024.2338539>
477
7. Mrak M., Winnefeld F., Lothenbach B., et al. (2021) "The influence of calcium sulfate content on the hydration of belite-calcium sulfoaluminate cements with different clinker phase compositions," *Materials and Structures*, vol. 54, no. 212.
480 <https://doi.org/10.1617/s11527-021-01811-w>

- 483 8. Sun F., Pang X., Wei J., et al. (2023) Synthesis of alite, belite and ferrite in both
monophase and polyphase states and their hydration behavior. *Journal of Materials
Research and Technology*, vol. 25, p. 3901–3916. <https://doi.org/10.1016/j.jmrt.2023.06.151>
- 486 9. Boháč M., Krejčí Kotlánová M., Kubátová D., et al. (2024) “Low Energy Alite and Belite-
Rich LC3: Early Hydration, Isothermal Calorimetry and Strength Development,”
489 *Proceedings of the 7th International Conference on Geotechnics, Civil Engineering and
Structures, CIGOS 2024*, p. 509–517. https://doi.org/10.1007/978-981-97-1972-3_56
- 492 10. Cába V., Sedlačík M., Iliushchenko V., et al. (2022) “Belite-Rich Cement - A more
Environmentally Friendly Alternative to Ordinary Portland Cement,” *Solid State
Phenomena*, vol. 337, p. 123–128. <https://doi.org/10.4028/p-ap8m7g>
- 495 11. Khankhaje E., Kim T., Jang H., et al. (2024) “A review of utilization of industrial waste
materials as cement replacement in pervious concrete: An alternative approach to
sustainable pervious concrete production,” *Heliyon*, vol. 10, no. e26188.
<https://doi.org/10.1016/j.heliyon.2024.e26188>
- 498 12. Rivera Sasso O., Carreño Gallardo C., Soto Castillo D.M., et al. (2024) “Valorization of
Biomass and Industrial Wastes as Alternative Fuels for Sustainable Cement Production,”
Clean Technologies, vol. 6, p. 814–825. <https://doi.org/10.3390/cleantechnol6020042>
- 501 13. Nandhini K., Karthikeyan J., (2022) “Influence of Industrial and Agricultural By-Products
as Cementitious Blends in Self-Compacting Concrete – A Review,” *Silicon* vol. 14, p. 2431–
2452. <https://doi.org/10.1007/s12633-021-01043-1>
- 504 14. Zanolli S.M., Orlietti L., Cocchioni F., et al. (2021) “Optimization of the Clinker
Production Phase in a Cement Plant,” *Proceeding of CONTROLO*, p. 263–273.
https://doi.org/10.1007/978-3-030-58653-9_25
- 507 15. Albrektienė-Plačakė R., Bazienė K., Gargasas J., (2023) “Investigation on Applying
Biodegradable Material for Removal of Various Substances (Fluorides, Nitrates and Lead)
from Water,” *Materials*, vol 16, no. 6519. <https://doi.org/10.3390/ma16196519>
- 510 16. Kognole A.A., Aytenfisu A.H., MacKerell A.D., (2020) “Balanced polarizable Drude force
field parameters for molecular anions: phosphates, sulfates, sulfamates, and oxides,”
Journal of Molecular Modeling, vol. 26, no. 152.
<https://doi.org/10.1007/s00894-020-04399-0>
- 513 17. Kwon W.T., Kim Y., Lee Y.J., et al. (2009) “Effects of Pair-Mineralizer on Burnability of
Clinker and Formation of Mineral,” *Materials Science Forum*, vol. 620–622, p. 209–212.
<https://doi.org/10.4028/www.scientific.net/MSF.620-622.209>
- 516 18. Siddique R., Khan M.I., (2011) “Supplementary Cementing Materials,” *Engineering
Materials book series, Springer* <https://doi.org/10.1007/978-3-642-17866-5>
- 519 19. Juenger M.C.G., Snellings R., Bernal S.A., (2019) “Supplementary cementitious
materials: New sources, characterization, and performance insights,” *Cement and Concrete
Research*, vol. 122, p. 257–273. <https://doi.org/10.1016/j.cemconres.2019.05.008>

20. Olowofoyeku A.M., Ofuyatan O.M., Oluwafemi J., et al. (2019) "Effect of Superplasticizer on Workability and Properties of Self-Compacting Concrete," *Journal of Physics: Conference Series*, vol.1378, no. 042088. <https://doi.org/10.1088/1742-6596/1378/4/042088>
21. Moodi F., Kashi A., Ramezani-pour A.A., et al. (2018) "Investigation on mechanical and durability properties of polymer and latex-modified concretes," *Construction and Building Materials*, vol. 191, p.145–154. <https://doi.org/10.1016/j.conbuildmat.2018.09.198>
22. Wang Z., Xu J., Xia W., et al. (2020) "Research on Interfacial Bonding Properties and Engineering Applications of Polymer Modified Mortar," *E3S Web of Conferences*, vol. 198, no. 01045. <https://doi.org/10.1051/e3sconf/202019801045>
23. Cao Q.Y., Hao T.Y., Sun W., (2013) "Study on Polymer-Modified Concrete for Improving Flexural Toughness," *Applied Mechanics and Materials*, vol. 405–408, p. 2815–2819. <https://doi.org/10.4028/www.scientific.net/AMM.405-408.2815>
24. Yamashita M., Tanaka H., Sakai E., et al. (2019) "Mineralogical study of high SO₃ clinker produced using waste gypsum board in a cement kiln," *Construction and Building Materials*, vol. 217, p. 507-517. <https://doi.org/10.1016/j.conbuildmat.2019.05.098>
25. Bentur A., (1976) "Effect of Gypsum on the Hydration and Strength of C3S Pastes," *Journal of the American Ceramic Society*, vol. 59, p. 210–213. <https://doi.org/10.1111/j.1151-2916.1976.tb10935.x>
26. Soroka I., Abayneh M., (1986) "Effect of gypsum on properties and internal structure of PC paste," *Cement and Concrete Research*, vol. 16, p. 495–504. [https://doi.org/10.1016/0008-8846\(86\)90087-6](https://doi.org/10.1016/0008-8846(86)90087-6)
27. Yamaguchi G., Takemoto K., Uchikwa H., Takagi S., (1961) "On the influence of gypsum upon the rate of hydration of portland cement," *Journal of the Ceramic Association* vol. 69, p. 112–125. <https://doi.org/10.2109/jcersj1950.69.112>
28. Aksan U., Köseoğlu K., Çelik M.S., (2021) "Enhancing burnability characteristics of low-temperature burnt-cement clinker by recycling phosphogypsum wastes," *Journal of Materials in Civil Engineering*, vol. 33(9), no. 04021250. [https://doi.org/10.1061/\(ASCE\)MT.1943-5533.0003786](https://doi.org/10.1061/(ASCE)MT.1943-5533.0003786)
29. Tserenkhand B., Sanjaasuren R., Solongo P., (2014) "Composition of iron ores from Mongolian western region and its applicability for cement production," *Mongolian Journal of Chemistry*, vol. 14, p. 75–79. <https://doi.org/10.5564/mjc.v14i0.204>
30. Pérez-Bravo R., Álvarez-Pinazo G., Compañá J.M., et al. (2014) "Alite sulfoaluminate clinker: Rietveld mineralogical and SEM-EDX analysis," *Advances in Cement Research*, vol. 26, p. 10–20. <https://doi.org/10.1680/adcr.12.00044>
31. Lerch W.M., Bogue R.H., (1926) "Determination of Uncombined Lime in Portland Cement," *Industrial and Engineering Chemistry*, vol.18, p. 739–743. <https://doi.org/10.1021/ie50199a022>

32. Mache E., Rajczakowska M., Cwirzen A., (2025) "Process Residues in Cement Clinker Production: A Review," *Waste Management Bulletin*, vol. 3, no. 100205.

561

<https://doi.org/10.1016/j.wmb.2025.100205>

33. Taylor H.F.W., (1997) "Cement chemistry" (2nd edition). *Thomas Telford Publishing*, p. 0–470, <https://doi.org/10.1680/cc.25929>

564

34. Kacimi L., Simon-Masseron A., Ghomari A., et al. (2006) "Reduction of clinkerization temperature by using phosphogypsum," *Journal of Hazardous Materials*, vol. 137, p. 129–137. <https://doi.org/10.1016/j.jhazmat.2005.12.053>

567

35. Tobón J.I., Díaz-Burbano M.F., Restrepo-Baena O.J., (2016) "Optimal fluorite/gypsum mineralizer ratio in Portland cement clinkering," *Materiales de Construcción*, vol. 66, p. e086–e086. <https://doi.org/10.3989/mc.2016.05515>

570

36. Raina K., Janakiraman L.K., (1998) "Use of mineralizer in black meal process for improved clinkerization and conservation of energy," *Cement and Concrete Research*, vol. 28, p. 1093–1099. [https://doi.org/10.1016/S0008-8846\(98\)00082-9](https://doi.org/10.1016/S0008-8846(98)00082-9)

573

37. Idris M.S., Ismail K.N., Jamaludin S.B., et al. (2007) "Comparative Characterization of Clinker's Microstructure at Different Temperature Zone during Cement Production," *American Journal of Applied sciences*, vol. 4, p. 543–546.

576

<https://doi.org/10.3844/ajassp.2007.543.546>

38. Benmohamed M., Alouani R., Jmayai A., et al. (2016) "Morphological Analysis of White Cement Clinker Minerals: Discussion on the Crystallization-Related Defects," *International Journal of Analytical Chemistry*, vol. 2016, p. 1259094.

579

<https://doi.org/10.1155/2016/1259094>

39. Mongolian Agency for Standardization and Metrology (2008) "MNS974: 2008 Portland Cement Technical Requirements" Ulaanbaatar: Agency for Standardization and Metrology.

582